Journal of Great Lakes Research 48 (2022) 1710–1717

Contents lists available at ScienceDirect

Journal of Great Lakes Research

journal homepage: www.elsevier.com/locate/ijglr

Satellite based lake bed elevation model of Lake Urmia using time series of Landsat imagery

Tanja Schröder [a,*], Elmira Hassanzadeh [b], Sahand Darehshouri [a], Massoud Tajrishy [c], Stephan Schulz [a]

[a] Technische Universität Darmstadt, Institute of Applied Geosciences, Schnittspahnstr. 9, 64287 Darmstadt, Germany
[b] Polytechnique Montréal – Department of Civil, Geological and Mining Engineering, Montreal, Canada
[c] Sharif University of Technology, Urmia Lake Restoration Program, Department of Civil Engineering, Azadi Ave, P.O. Box: 11155, 9313 Tehran, Iran

ARTICLE INFO

Article history:
Received 17 November 2021
Accepted 3 August 2022
Available online 26 August 2022
Communicated by Caren Binding

Keywords:
Lake Urmia
Remote sensing
Bathymetry
GIS
NDWI
Level-Area-Volume relationship

ABSTRACT

This study presents a lake bed elevation model of Lake Urmia. In the course of model generation, a time series of the extent of the lake surface was derived from 129 satellite images with different acquisition dates based on the Landsat sensors Thematic Mapper (TM), Enhanced Thematic Mapper Plus (ETM+), and Operational Land Imager (OLI). Due to the rapid shrinking of the lake during the last two decades, lake surface areas ranging from 890 km^2 to 6125 km^2 could be covered. The water edge of the various lake extents was then linked to the observed water level on the day of the satellite image acquisition. The resulting contour lines, covering water levels between 1270.04 m and 1278.42 m a.s.l. and thus representing the lakebed morphology in its shallow parts, were merged with existing data (deeper parts) and interpolated to generate a lake bed elevation model. Finally, Lake Urmia's Level-Area-Volume relationships were derived from the lake bed elevation model and compared to bathymetric data previously published.

Introduction

Lake Urmia, located in northwest Iran (Fig. 1), is one of the largest hyper-saline lakes in the world (AghaKouchak et al., 2015; Sima and Tajrishy, 2013). Over the past few decades, the lake's water level has dropped significantly (Karimi et al., 2016; Golabian, 2011; Wurtsbaugh et al., 2017; Sima et al., 2021). In particular, between 1995 and 2013 the lake lost about 60 % of its area and more than 90 % of its volume (Schulz et al., 2020). Such a drastic reduction has not been observed in past centuries and can therefore most likely not only be attributed to natural climate variability (Alborzi et al., 2018). Intense human activities in upstream regions (e.g., agricultural developments and construction of reservoirs), changes in climate, as well as mismanagement of water resources are the key contributors to this issue (Jeihouni et al., 2017; Schulz et al., 2020; S. Sima and Tajrishy, 2013; Talebi et al., 2016; Tourian et al., 2015). Although recently the lake's water level has slightly increased (ULRP, 2021a), it is still about four meters below the critical threshold (1274.1 m), which marks the water level that must be reached in order to restore the lake's natural ecology (ULRP, 2021a).

The morphology of Lake Urmia is characterized by shallow coastal areas and gradually deepening central parts with a maximum depth of about 9 m below the average historical level of the lake (1965–1995). This specific morphology results in a strong response of lake area to water level, i.e., small changes in water level (or volume) causes large changes in surface area. In turn, changes in the extent of the lake affect the total evaporation amount, which constitutes the only relevant outflow component of the lake (JICA, 2016; Water Research Institute, 2003). Therefore, precise information about the lake's bathymetry is required to study highly dynamic hydrological processes such as precipitation input and evaporative loss from the lake's surface and to thus understand the lake's water budget.

Sima et al. (2021) presented a set of measurable restoration objectives for Lake Urmia. Among other things, they propose to investigate where and when land bridges may form to the islands, as these may pose a threat to endemic mammals living there due to exposure to predators. Accurate bathymetric data on the shallow parts of the lake can help to make more reliable predictions in this context. It is also important to note that the enormous recession of the lake has led to a strong concentration of dissolved salts, eventually resulting in salt precipitation. These precipitates change the morphology of the lake bed, which makes it necessary

* Corresponding author.
E-mail address: tanja.schroeder@ufz.de (T. Schröder).

https://doi.org/10.1016/j.jglr.2022.08.016

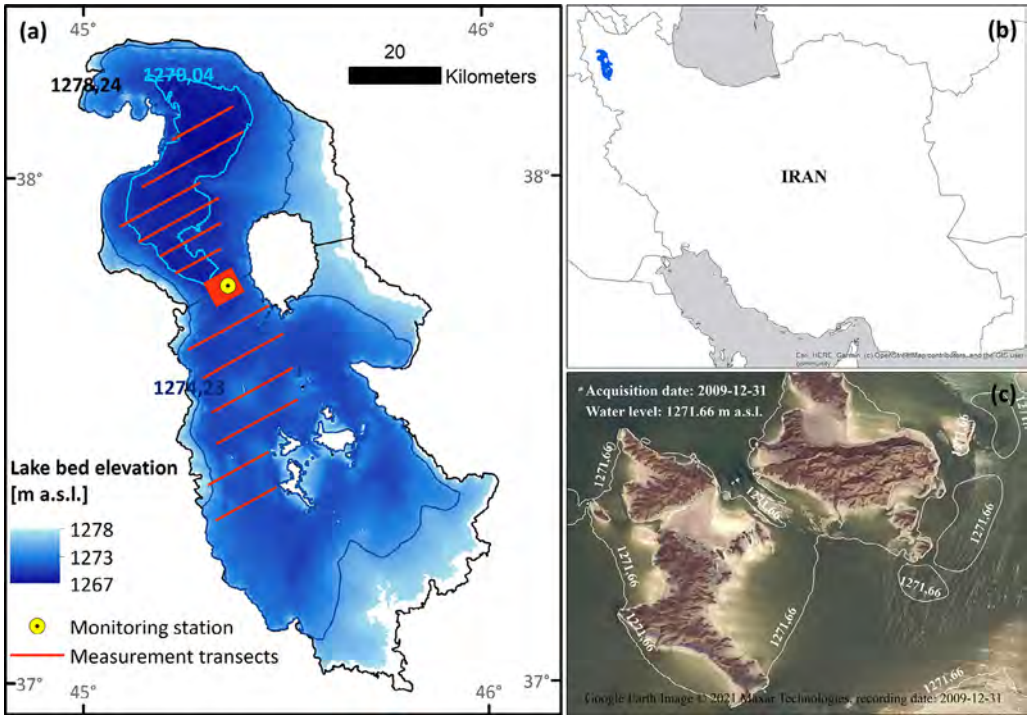

Fig. 1. (a) Former bathymetric data of Lake Urmia and measurement transects of the ship-based echo sounding campaign, conducted by the Ministry of Energy's Water Research Institute; (b) overview map; and (c) true color satellite image from 2009-12-31 of the southern islands and 1271.66 m a.s.l. contour line of the former bathymetric data (corresponds to the water level on 2009-12-31).

to check and, if necessary, adjust the bathymetry from time to time (Sima et al., 2021).

The Urmia Lake Restoration Program (ULRP) commissioned an echo sounding survey conducted by the Ministry of Energy's Water Research Institute (IWRMC) in 2017. Based on these water depth measurements a bathymetry of Lake Urmia was further improved. However, a comparison of the lake's actual water edge, visible on true color satellite images, and the theoretical one derived from the recent bathymetric data combined with water level records (white contour line, Fig. 1c) revealed some inaccuracies of the recent bathymetry in the shallow parts of the lake such as elevations being too high around the southern islands (Fig. 1c). Therefore, the objective of this study is to improve the understanding of the lake bed elevation by incorporating satellite-based remote sensing derived data from shallower locations of the lake.

Bathymetric data can be translated into Level-Area-Volume (LAV) relationships (sometimes also referred to as rating curves), which constitutes a practical tool, frequently used in water balance studies (Hassanzadeh et al., 2012; Jeihouni et al., 2017; Schulz et al., 2020). Level-Area-Volume relationships for Lake Urmia were provided by WRI (2005). Furthermore, WWA/Yekom (2005) and Jeihouni et al. (2017) presented a set of mathematical functions to describe these rating curves. In addition, Karimi et al. (2016) developed a bathymetric model of Lake Urmia, from which rating curves were derived. Level-area-volume relationships were also determined by Sima and Tajrishy (2013) using remote sensing data and analytical models. In this study we aim to derive LAV-relationships from the developed lake bed elevation model and compare them to previously published ones.

Study area

The Lake Urmia basin encompass high mountains such as the Kuh-e Sahand with an elevation of 3,710 m a.s.l., as well as large agriculturally used plains, e.g., around the cities of Miandoab, Urmia, and Tabriz. According to the Köppen-Geiger classification system, the climate in the basin is generally classified as semi-arid (Kottek et al., 2006). The maximum surface area of the Lake Urmia was observed in 1995 and was estimated to be approximately 6,100 km^2 (Eimanifar and Mohebbi, 2007). During the time of its greatest expansion, the lake was about 140 km long and 40–55 km wide (Delju et al., 2013). About 60 rivers (17 permanent and 12 seasonal rivers, and 39 floodways) exist in the Lake Urmia Basin (Hashemi, 2008) and are the main source of lake water. From 1967 to 2015 several reservoirs with total capacity of 2.2 km^3 were built in this area to supply water for socio-economic activities, mostly irrigated agriculture (Schulz et al., 2020). The annual inflow to the lake is characterized by strong interannual fluctuations, ranging between 0.5 and 14.5 km^3a^{-1} from 1954 to 2017. Precipitation over the lake is another source of water, averaging 1.5 km^3a^{-1} during the same observation period. As mentioned above, with an average of 4.9 km^3a^{-1} (1954–2017), evaporation from the lake surface is the most important relevant outflow component of this endorheic lake (Schulz et al., 2020). The groundwater component of the lake's water balance is estimated to be relatively small (Amiri et al., 2016; Hasemi, 2011; Shadkam et al., 2016). Due to reduction of surface water inflow and high evaporation rates in the recent past, a large amount of salt has been deposited in the lake and on the dried-up lake bed (Jeihouni et al., 2017).

Methods and data

For referencing of the lake bed elevation model, Landsat satellite imagery was first classified into water and land to extract the water edges of the lake. Subsequently, these water edges were combined with recorded water levels to generate contour lines describing the lakebed above 1,270.04 m a.s.l. These contour lines were merged with existing data (ULRP, 2018), covering water levels ranging from 1,267.1 m to 1,270.04 m a.s.l., to develop the intended lake bed elevation model.

In situ measurements (existing data)

As previously noted, water depth was measured in 2017 along various transects according to the international standard S-44 for hydrographic surveys (IHO, 2008). For combining and processing the data from the Differential-GPS (Ashtech DG14) and the echo sounder (CEEDUCER, Hydrotrac II) the Hypack software was used. Measured transects were distributed well over the deeper parts of the lake, and thus lake bed elevations between approximately 1,267 m and 1,274.23 m a.s.l. were captured. The transects near the bridge were 500 m apart (Fig. 1a). Due to the 50 cm draft of the boat used for the echo sounder campaign, shallow areas of the lake were not accessible (ULRP, 2018). Using the water depth data in combination with previous information, a bathymetry of Lake Urmia with a resolution of 30 × 30 m was obtained capturing elevations from 1,267 to 1,278 m (ULRP, 2018).

In addition, Lake Urmia's water level has been measured continuously by the Urmia Lake Restoration Program and the Ministry of Energy's Water Research Institute since 1965 at the monitoring station depicted in Fig. 1a (ULRP, 2021b). The period between 1995 and 2015 covers the entire range of observed water level data with a maximum of 1,278.41 m (1995) and a minimum of 1,270.04 m (2015). Water levels before 1995 and after 2015 remained in this range.

Satellite images

In order to delineate the lake's water surface area, 129 (one or a set of two neighboring scenes; Electronic Supplementary Material (ESM) Table S1; example image given in ESM Fig. S1). Landsat satellite images with acquisition dates, covering a period from 1995 to 2015, were acquired via the U.S. Geological Survey's Earth Explorer (U.S. Geological Survey, 2021). Of these images 95, 16, and 18 originate from Landsat TM, ETM + and OLI sensors respectively. The primary selection criteria were to obtain images that are cloud-free and cover almost all of the lake's surface. Moreover, a good coverage of water levels between 1,270.04 m and 1,278.42 m a.s.l. with approximately 0.1 m intervals was required. This is the minimum vertical resolution due to the number of available satellite images. For most parts of the lake a 30x30m Landsat pixel allows for the separation of these water levels because the horizontal distance between two contour lines is almost always greater than 30 m. Only at one part of the shoreline of Lake Urmia a 0.1 m water level difference would be hard to capture due to too steep lake bed gradients, i.e., the horizontal distance between the highest (1,278.4 m) and lowest point (1,270.7 m) is only about 100 m.

Most of the selected images for our study have a good quality with a cloud cover of less than 10 %. At higher water levels the available images do not cover the entire lake surface. Therefore, besides the 129 images, 41 additional images were obtained to complement the scenes. These paired images are not always taken on the same date, but at a date with similar or identical water level.

The acquired Landsat images are Level1-Terrain-Corrected (L1T) and consist of seven (TM/ETM +) or eleven (OLI) spectral bands with a spatial resolution of 30 m for the optical bands (U.S. Geological Survey, 2020).

Data processing

The data processing procedure is illustrated in Fig. 2. The obtained satellite scenes were pre-processed by clipping, mosaicking and generating true color images. The water surface area was extracted from the mosaicked scenes using a thresholding approach, either based on the Normalized Difference Water Index (NDWI; McFeeters, 1996) or the Modified Normalized Difference Index (MNDWI; Xu, 2006) in combination with the red band. The NDWI (Eq. (1)) and MNDWI (Eq. (2)) were calculated, using the green band in combination with the near infrared (NIR) or the shortwave infrared band (SWIR).

$$NDWI = \frac{Green - NIR}{Green + NIR} \quad (1)$$

$$MNDWI = \frac{Green - SWIR}{Green + SWIR} \quad (2)$$

Based on these indices, the scenes were reclassified to water and land using individually determined threshold values for each image (Fig. 2). The reclassified binary raster images were compared to the corresponding true color images to determine whether the NDWI or the MNDWI better describes the water area. For most scenes, the NDWI was found to extract the surface area better based upon visual examination. If salt deposits along the coast lines were misclassified as water, the red band, as it was found to be the most suitable band to distinguish between salt deposits and water, was reclassified and subtracted from the NDWI. Every pixel, classified as water by the NDWI, was changed into land as long as the same pixel was classified as land by the red band. For some scenes with a corresponding water level of more than 1,275.7 m a.s.l. the NDWI underestimated the water area at the eastern part of the coast. In these cases, the MNDWI, from which the red band was subtracted as described above, was used (Fig. 3). Morphological operations (dilation and erosion) and, subsequently, a low pass filter were applied for noise reduction. These operations are strongly influenced by size and shape of the kernel as well as the number of iterations. Generally, the shape of the kernel depends on the geometric shape of the objects of interest (Padghan, 2019). For satellite images, oriented or rectangular kernels are recommended (Padghan, 2019). The size of the kernel depends on the size of the object of interest in the image (Padghan, 2019). Because the preservation of finer structures of the coastline is important a small kernel was used. Several rectangular kernels of different sizes were created manually with help of NumPy. The morphological operations were executed using Cv2 operations from OpenCV. Different numbers of iterations were tested. A 3 × 3 kernel was finally applied performing 10 iterations for each operation.

The binary raster images, classified into water and land, were then converted into line features, representing the water edges of the lake. Based on the acquisition dates of the corresponding satellite images, each water edge was then assigned an elevation from the lake level records. Afterwards, these lines, attributed with an elevation, were smoothed to facilitate interpolation and then combined into a set of contour lines covering water levels between 1,270.4 m and 1,278.4 m a.s.l. The former bathymetric information was used to add morphological information of the lakebed below 1,270.04 m a.s.l. Thus, contour lines were derived from the former bathymetry with an interval of 0.1 m. The merged set of contour lines was interpolated to create a Triangulated Irregular Network (TIN) dataset. A TIN dataset is a vector-based data model constructed by triangulating vertices or data points. Delaunay triangulation was applied for interpolation to form the non-overlapping triangles (with 3D coordinates) that cover the entire area of interest. Finally, the TIN dataset was converted into a raster, which represents the intended lake bed elevation model.

LAV-relationships were derived from the generated TIN dataset. Area and volume were calculated using a reference plane of a constant elevation. The reference plane was intersected with the surface of the TIN dataset and the area in common was determined. The surface area was calculated for all triangles (and parts of intersected triangles) that are located inside of the intersected polygon. Furthermore, the volume below the reference plane was determined. The calculations were only applied for elevations below

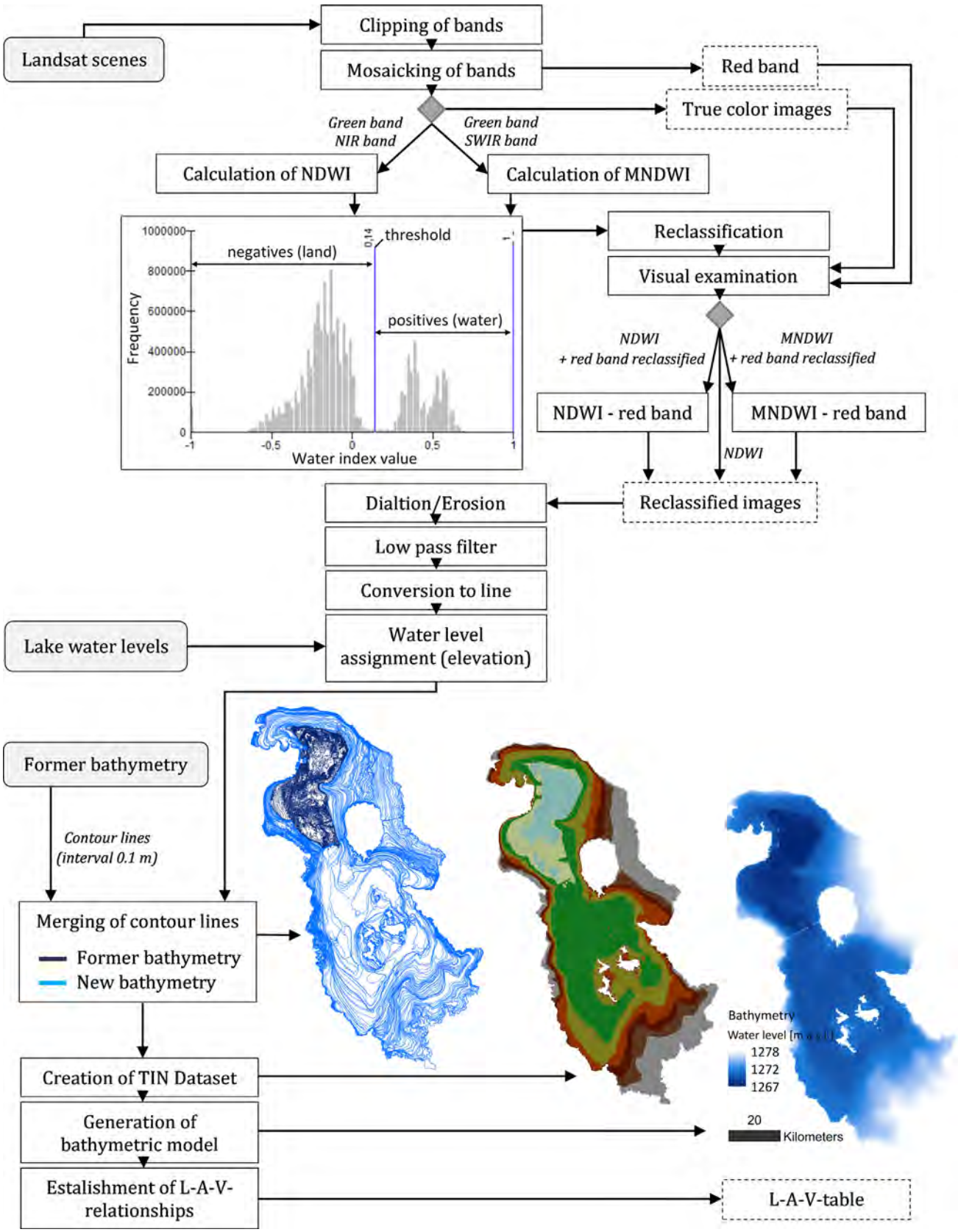

Fig. 2. Data processing flowchart.

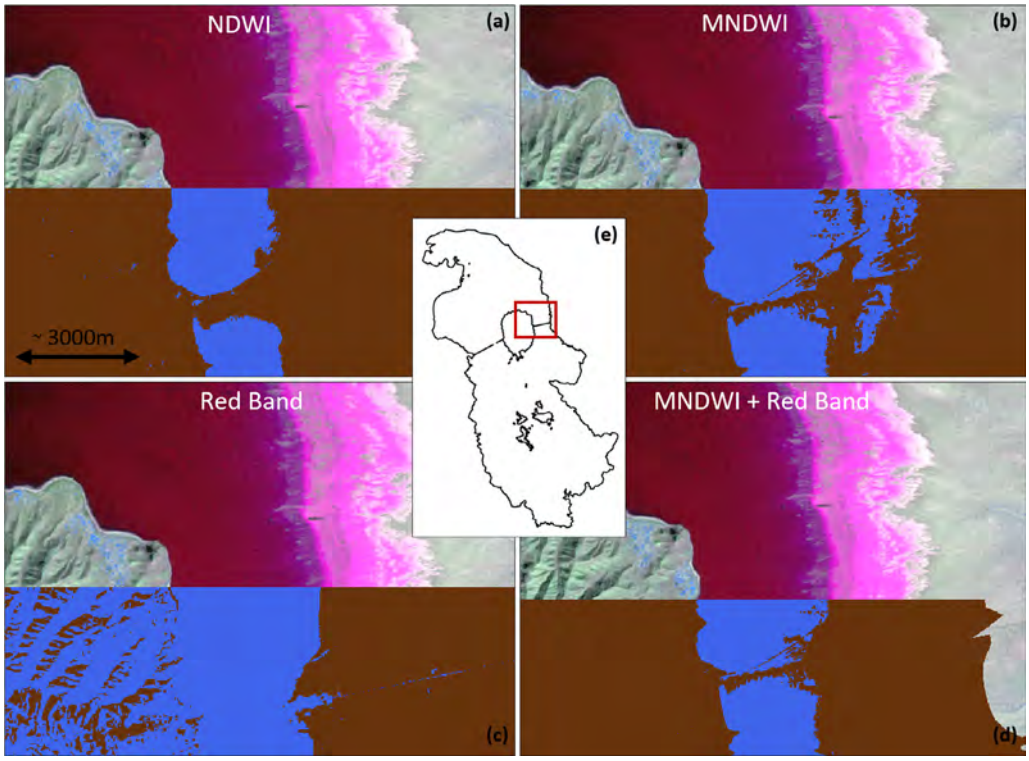

Fig. 3. Fig. 1: (a) Reclassified image by NDWI; (b) reclassified image by MNDWI; (c) reclassified image by red band; and (d) reclassified image by MNDWI and red band compared to the RGB composite image from 1998-10-12; (e) overview map. (For interpretation of the references to color in this figure legend, the reader is referred to the web version of this article.)

or equal to 1,278.4 m. An elevation interval of 0.1 m was applied. All operations were executed using functions available in ArcGIS (version 10.7.1). A Matlab script (ESM Appendix S1) was used to determine surface area and volume from lake bed elevation model and water level.

Impact of salt deposits

With the decline of the lake water level, a concentration of the dissolved salts occurs, which leads to precipitation of the salts when the water level falls below a certain level. These precipitates have an influence on the morphology of the dried up lake bed and the consideration of this influence might be relevant to various management and research questions. For example, not accounting for salt precipitation may lead to the assumption that land bridges to the islands are formed at a lower water level than is actually the case. In contrast to a classical bathymetric model based on depth measurements below the lake surface, in this this study, we developed an elevation model of the dried up lake bed based on actual satellite observations of the water edge. It thus includes salt precipitation and is therefore useful for predicting the actual lake area evolution.

Nevertheless, we are interested in an estimate of the thickness and spatial extent of the salt precipitation and have therefore conducted further investigations. For this purpose, we first determined from a series of measured values for water level and salinity (Karbassi et al., 2010) at which water level the salt saturation of the lake is reached. Since the salt concentration of Lake Urmia is higher in the northern part than in the southern one, we have distinguished two different cases. For the first case, we assumed that the salt concentration in the northern part corresponds to the average of the lake, from which a lower limit for the water level at saturation could be derived. For the second case, on the other hand, we assumed that the salt concentration in the north is 21 g/l higher (the largest observed difference) than the average. From this assumption, a maximum water level at saturation could be estimated (Fig. 4a). Using the existing bathymetric model (ULRP, 2018), we were able to determine the volume of the lake at these water levels and thus the total mass of the dissolved salts. With a further decrease in the lake water level, we have made the simplifying assumption that the excess salt precipitates evenly over the remaining lake area. These analyses allowed us to estimate the spatial extent (Fig. 4d) of the salt deposits and their average thickness (Fig. 4e). Observations made during a field campaign in March 2018 support these findings. A photo of the dried up lake bed above the water level of salt saturation, for example, shows that there is only a very thin film of salt on the clastic and biogenic sediments (Fig. 4b). In contrast, another photo, taken at a location below the water level of salt saturation, clearly shows a few centimeters of salt precipitates (Fig. 4c).

Results

The generated lake bed elevation model shows that the lake is shallow with a maximum depth is only about 11.3 m (below 1,278.4 m a.s.l.). The deepest part of the lake is located in the north at an elevation of approximately 1,267.1 m a.s.l. For the southern part, the deepest point is at an elevation of 1,270.11 m a.s.l. In the south the lake's shore is flat and has a very gentle slope. Similarly, the lake's shore in the northeast is rather flat, descending slowly. The rest of the lake's shore is somewhat steeper. The morphology of the lakebed in the northern part is more homogenous, with the deepest point located approximately in the middle. The southern and northern part of the lake a separated through a causeway with an opening of about 1,280 m in length.

The elevation difference between our lake bed elevation model and the previously developed bathymetry by ULRP was determined by subtracting the former bathymetry from our lake bed

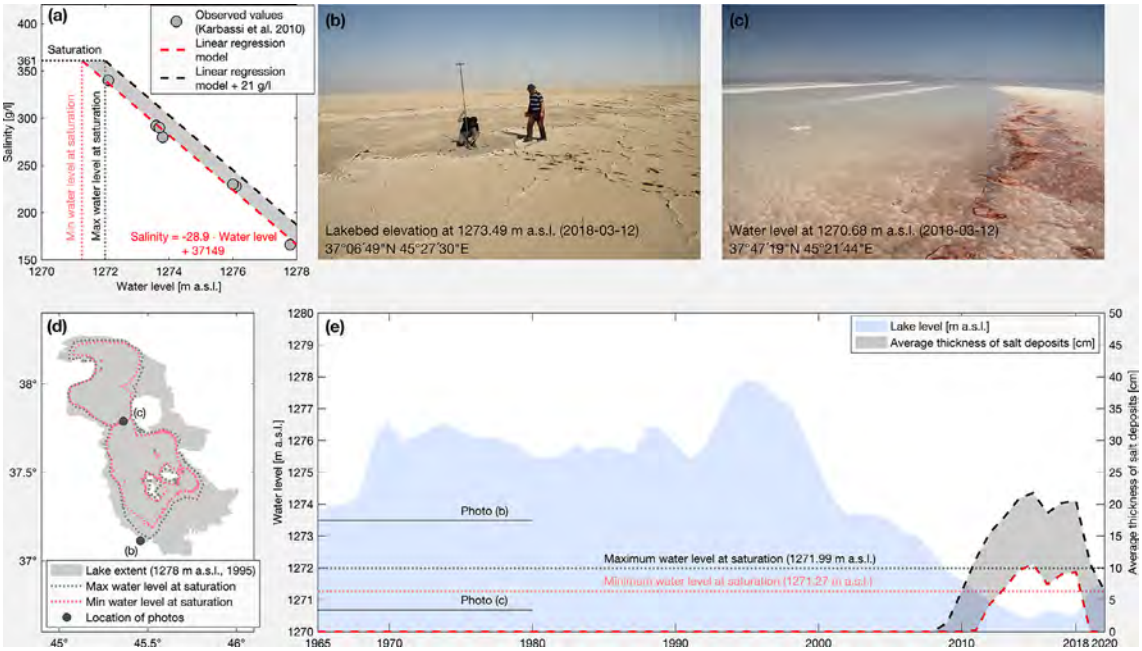

Fig. 4. (a) Water level-salinity relationship (Karbassi et al., 2010); (b) and (c) photos of the lake bed taken on 2018–03-12; (d) lake extent at saturation; (e) temporal evolution of water level and average thickness of salt deposits.

elevation model (Fig. 5a). For the shallow areas, especially surrounding the southern islands and the northwest shore of the lake, an elevation difference of up to 5.9 m was detected. Two high resolution true color satellite images (Google Earth) of a bay in the northern part of the lake and the southern islands were used to compare the corresponding contour lines of our lake bed elevation model as well as the former bathymetry to the image (Fig. 5c and Fig. 5d). The figures show that the shallow areas are better represented by our lake bed elevation model. In addition, a high-resolution true color image (Google Earth) from the eastern water edge was compared to the corresponding contour lines of our lake bed elevation model and the former bathymetry to analyze the elevation difference at the interface between satellite derived data and ULRP bathymetric data (Fig. 5a). This example demonstrates that our lake bed elevation model, generally, slightly underestimates the water surface area. Whereas the bathymetric data by ULRP tends to overestimate the water surface area in this part of the lake.

The rating curves obtained from the lake bed elevation model show a reduction of 86 % of the lake's surface area and 95 % of its volume between 1995 and 2015 (Fig. 6a and Fig. 6b). The minimum and maximum surface area, that were observed at water

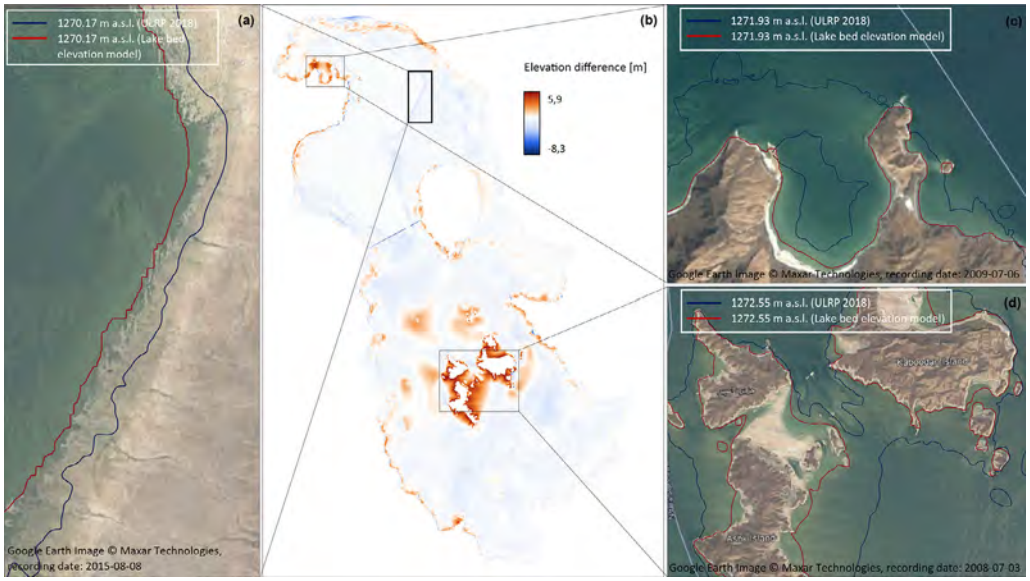

Fig. 5. (a) true color satellite image from 2015-08-08 of the eastern water edge and 1270.17 m a.s.l. contour lines of the lake bed elevation model and the ULRP bathymetric data (corresponds to the water level on 2015-08-08);(b) elevation difference between our lake bed elevation model and bathymetry developed in 2017 by ULRP; (c) true color satellite image from 2009-07-06 of a bay in the northern part of Lake Urmia and 1271.93 m a.s.l. contour lines of the lake bed elevation model and the ULRP bathymetric data (corresponds to the water level on 2009-07-06); (d) true color satellite image from 2008-07-03 of the southern islands and 1272.55 m a.s.l. contour lines of the lake bed elevation model and the ULRP bathymetric data (corresponds to the water level on 2008-07-03).

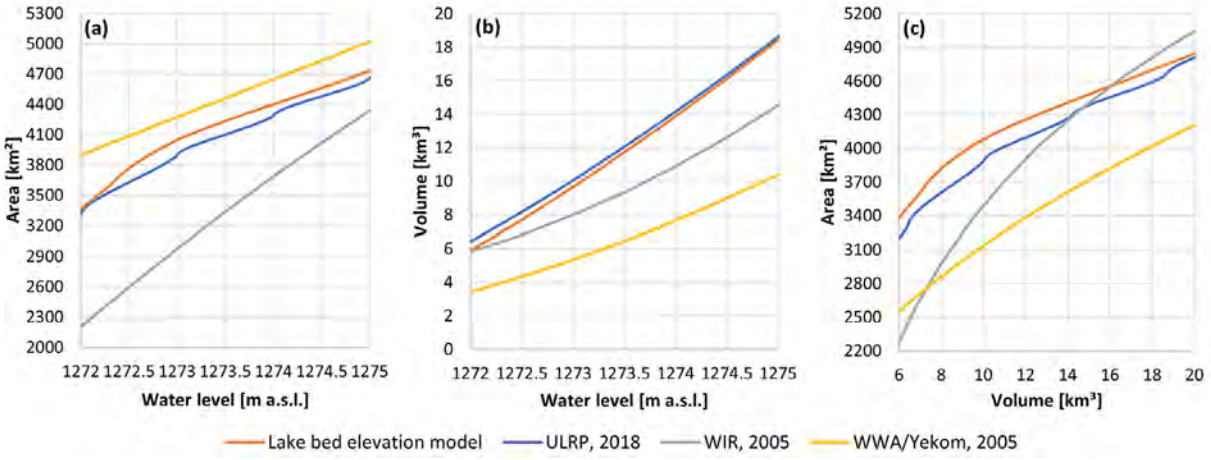

Fig. 6. Lake Urmia relationships between (a) Level and Area, (b) Level and Volume, and (c) Volume and Area, derived from the combined bathymetric model, developed in this study (red), the former bathymetric model based on the echo sounding campaign (blue; IWRMC, 2017) as well as those established by WIR (2005) and WWA/Yekome (2005) in green and light blue, respectively. (For interpretation of the references to color in this figure legend, the reader is referred to the web version of this article.)

levels of 1,270.04 m and 1,278.4 m, amount to 862.24 km2 and 6,122.88 km2, respectively, with corresponding volumes of 1.36 km3 and 36.81 km3. There is a non-linear relationship between water level, surface area and volume due to lake's morphology. The curve depicting the relationship between water level and surface area is steeper between water levels of 1,271.0 m and 1,274.5 m (Fig. 6a). Above and below this range the reaction of the surface area to the water level is less pronounced. The curve, describing the relationship between water level and volume, initially ascends slightly, but becomes steeper above a water level of 1,271 m. A volume of 1.3 km3 constitutes a tipping point of the rating curve between volume and surface. This point is reached when the shallow southern part of the lake falls completely dry. Above this point and up to a volume of 9 km3, small changes in volume cause large alterations in surface area with an increase in area of about 400 km2 for every additional cubic kilometer of lake water. In comparison, above this volume an increase in volume of 1 km3 leads, on average, to an increase in surface area of about 75 km2. According to our findings salt precipitation starts to occur at water levels of 1,271.27–1,271.99 m a.s.l.

Comparison of LAV-relationships

The LAV-relationships obtained based on the lake bed elevation model are utilized to update the rating curves for Lake Urmia. Therefore, the rating curves were compared with those obtained on the basis of the bathymetric data by ULRP (2018) as well those established by WIR (2005) and WWA/Yekome (2005) based on data prior to 2005. The shape of the rating curves derived from the lake bed elevation model is relatively similar to those derived from the bathymetric data by ULRP (Fig. 6). Due to differences in the models regarding the shallow areas of the lake, the surface area as defined by the lake bed elevation model is up to 170 km^2 larger between water levels of 1,271.9 m and 1,275 m compared to the bathymetric data by ULRP (Fig. 6a).

In comparison, LAV-relationships established by WIR (2005) and WWA/Yekomen (2005), which are obtained based on Lake Urmia's conditions prior to 2005, considerably deviate from the recent rating curves. This can be attributed to morphological changes in the lake bed over time, but also to less available data at the time. In addition, these relationships are expressed by first (surface area) or second (volume) order regression, which are not necessarily valid outside the range of the underlying meassurements.

Concluding remarks

The unfortunate circumstance that the lake level dropped had the positive side effect that the lake bottom was exposed and could thus be mapped with satellite data. To this end, the water surface area was extracted from the satellite images using a thresholding approach, combining NDWI, MNDWI as well as the reclassified Red Band (single band method). The corresponding water level was attributed to the extracted water surface area, resulting in contour lines describing the morphology of the dried-up lake bed. This remapping of the shallow areas of the lake (greater than1,274.04 m a.s.l.), which make up most of the lake area, resulted in a better representation of these areas with a maximum difference in surface area of approximately 170 km^2 (at a water level of 1272.8 m a.s.l.) compared to the bathymetric data provided by ULRP (2018).

The presented methodology can be applied to other shallow lakes that experienced strong fluctuations or reductions in water level over the past 30 years in Iran such as Lake Hamun or Lake Bakhtegan (Saemian et al., 2022) and other parts of the world such as Lake Chad, Aral Sea or the Great Salt Lake (Wurtsbaugh et al., 2017). The lake bed elevation model and rating curves can be used for various purposes, e.g. to estimate surface area and volume based on the measured water level (Using Matlab code found in ESM Appendix S1) or to simulate dynamically Lake Urmia's volume and water area which are required to calculate, e.g., evaporative loss and precipitation input. It can also be used by various national or international organizations such as the Urmia Lake Restoration Program (ULRP) for formulating objectives, indicators and measures to propose water management measures for Lake Urmia.

Declaration of Competing Interest

The authors declare that they have no known competing financial interests or personal relationships that could have appeared to influence the work reported in this paper.

Acknowledgement

Sahand Darehshouri acknowledges the support from the German Academic Exchange Service (DAAD) programme "Sustainable Water Management (NaWaM) Study Scholarsips and Research Grants 2015" (57156376) funded by the German Federal Ministry of Education and Research (BMBF).

Data availability

The lake bed elevation model of Lake Urmia is available from the PANGAEA database (https://doi.pangaea.de/10.1594/PANGAEA.938382).

Appendix A. Supplementary data

Supplementary data to this article can be found online at https://doi.org/10.1016/j.jglr.2022.08.016.

References

AghaKouchak, A., Norouzi, H., Madani, K., Mirchi, A., Azarderakhsh, M., Nazemi, A., Nasrollahi, N., Farahmand, A., Mehran, A., Hasanzadeh, E., 2015. Aral Sea syndrome desiccates Lake Urmia: Call for action. J. Great Lakes Res. 41 (1), 307–311. https://doi.org/10.1016/j.jglr.2014.12.007.

Alborzi, A., Mirchi, A., Moftakhari, H., Mallakpour, I., Alian, S., Nazemi, A., Hassanzadeh, E., Mazdiyasni, O., Ashraf, S., Madani, K., Norouzi, H., Azarderakhsh, M., Mehran, A., Sadegh, M., Castelletti, A., AghaKouchak, A., 2018. Climate-informed environmental inflows to revive a drying lake facing meteorological and anthropogenic droughts. Environ. Res. Lett. 13 (8), 84010. https://doi.org/10.1088/1748-9326/aad246.

Amiri, V., Nakhaei, M., Lak, R., Kholghi, M., 2016. Investigating the salinization and freshening processes of coastal groundwater resources in urmia aquifer, nw iran. Environ. Monit. Assess. 188 (4), 233. https://doi.org/10.1007/s10661-016-5231-5.

Delju, A.H., Ceylan, A., Piguet, E., Rebetez, M., 2013. Observed climate variability and change in Urmia Lake Basin, Iran. Theoretical Appl. Climatol. 111 (1–2), 285–296. https://doi.org/10.1007/s00704-012-0651-9.

Eimanifar, A., Mohebbi, F., 2007. Urmia lake (northwest iran): a brief review. Saline Systems 3, 5. https://doi.org/10.1186/1746-1448-3-5.

Golabian, H., 2011. Urumia lake: Hydro-ecological stabilization and permanence. In: Badescu, V., Cathcart, R.B. (Eds.), Environmental Science and Engineering. Macro-Engineering Seawater in Unique Environments. Springer Berlin Heidelberg, pp. 365–397. https://doi.org/10.1007/978-3-642-14779-1_18.

Hasemi, M., 2011. A socio-technical assessment framework for integrated water resources management (iwrm) in lake urmia basin, iran [PhD Thesis]. Newcastle University. http://hdl.handle.net/10443/1332

Hashemi, M., 2008. An independent review: The status of water resources in the lake uromiyeh basin: a synthesis report for the gef/undp conservation of iranian wetlands project. Newcastle University.

Hassanzadeh, E., Zarghami, M., Hassanzadeh, Y., 2012. Determining the main factors in declining the urmia lake level by using system dynamics modeling. Water Resour. Manage. 26 (1), 129–145. https://doi.org/10.1007/s11269-011-9909-8.

IHO, 2008. International Hydrographic Organization, IHO STANDARDS FOR HYDROGRAPHIC SURVEYS Special Publication No. 44 Published by the International Hydrographic Bureau MONACO 5th Edition, February 2008.

Jeihouni, M., Toomanian, A., Alavipanah, S.K., Hamzeh, S., 2017. Quantitative assessment of Urmia Lake water using spaceborne multisensor data and 3D modeling. Environ. Monit. Assess. 189 (11), 572. https://doi.org/10.1007/s10661-017-6308-5.

JICA, 2016. Data collection survey on hydrological cycle of Lake Urmia basin in the Islamic Republic of Iran.

Karbassi, A., Bidhendi, G.N., Pejman, A., Bidhendi, M.E., 2010. Environmental impacts of desalination on the ecology of Lake Urmia. J. Great Lakes Res. 36 (3), 419–424. https://doi.org/10.1016/j.jglr.2010.06.004.

Karimi, N., Bagheri, M.H., Hooshyaripor, F., Farokhnia, A., Sheshangosht, S., 2016. Deriving and evaluating bathymetry maps and stage curves for shallow lakes using remote sensing data. Water Resour. Manage. 30 (14), 5003–5020. https://doi.org/10.1007/s11269-016-1465-9.

Kottek, M., Grieser, J., Beck, C., Rudolf, B., Rubel, F., 2006. World map of the köppen-geiger climate classification updated. Meteorol. Z. 15 (3), 259–263. https://doi.org/10.1127/0941-2948/2006/0130.

McFeeters, S.K., 1996. The use of the normalized difference water index (ndwi) in the delineation of open water features. Int. J. Remote Sens. 17 (7), 1425–1432. https://doi.org/10.1080/01431169608948714.

Padghan, Abhishek Suresh (2019). Documentation For SRIP Project (Image processing lab - Morphological operations).

Saemian, P., Tourian, M., AghaKouchak, A., Madani, K., Sneeuw, N., 2022. How much water did Iran lose over the last two decades? J. Hydrol.: Reg. Stud. 41, (2022). https://doi.org/10.1016/j.ejrh.2022.101095 101095.

Schulz, S., Darehshouri, S., Hassanzadeh, E., Tajrishy, M [Massoud], and Schüth, C. (2020). Climate change or irrigated agriculture - what drives the water level decline of Lake Urmia. Scientific Reports, 10(1), 236. doi: 10.1038/s41598-019-57150-y.

Shadkam, S., Ludwig, F., van Oel, P., Kirmit, Ç., Kabat, P., 2016. Impacts of climate change and water resources development on the declining inflow into iran's urmia lake. J. Great Lakes Res. 42 (5), 942–952. https://doi.org/10.1016/J.JGLR.2016.07.033.

Sima, S [S.], and Tajrishy, M [M.] (2013). Using satellite data to extract volume–area–elevation relationships for Urmia Lake, Iran. J. Great Lakes Res., 39(1), 90–99. doi: 10.1016/j.jglr.2012.12.013.

Sima, S., Rosenberg, D.E., Wurtsbaugh, W.A., Null, S.E., Kettenring, K.M., 2021. Managing Lake Urmia, Iran for diverse restoration objectives: moving beyond a uniform target lake level. J. Hydrol.: Reg. Stud. 35, 100812.

Talebi, T., Ramezani, E., Djamali, M., Lahijani, H.A.K., Naqinezhad, A., Alizadeh, K., Andrieu-Ponel, V., 2016. The late-holocene climate change, vegetation dynamics, lake-level changes and anthropogenic impacts in the lake urmia region, nw iran. Quat. Int. 408, 40–51. https://doi.org/10.1016/j.quaint.2015.11.070.

Tourian, M.J., Elmi, O., Chen, Q., Devaraju, B., Roohi, S., Sneeuw, N., 2015. A spaceborne multisensor approach to monitor the desiccation of lake urmia in iran. Remote Sens. Environ. 156, 349–360. https://doi.org/10.1016/j.rse.2014.10.006.

U.S. Geological Survey. (2020). Landsat—Earth Observation Satellites. https://pubs.usgs.gov/fs/2015/3081/fs20153081_ver1.2.pdf.

U.S. Geological Survey. (2021). EarthExplorer: Landsat Imagery. https://earthexplorer.usgs.gov/.

ULRP. (2018). Urmia Lake Restoration Program and Ministry of Energy's Water Research Institute. Bathymetric data.

ULRP. (2021a). About Urmia Lake Basin. https://www.ulrp.ir/en/about-urmia-lake-basin/.

ULRP. (2021b). Urmia Lake Restoration Program. Lake level data. https://www.ulrp.ir/fa/.

Water Research Institute, 2003. Data Report. Integrated water resources management of Urmia Lake, Tehran.

WIR. (2005). Integrated Water Resources Management (IWRM) for Lake Uromyeh Basin. Iran (PvW-02.048). Ministry of Energy (MoE).

Wurtsbaugh, W.A., Miller, C., Null, S.E., DeRose, R.J., Wilcock, P., Hahnenberger, M., Howe, F., Moore, J., 2017. Decline of the world's saline lakes. Nat. Geosci. 10 (11), 816–821. https://doi.org/10.1038/NGEO3052.

WWA/Yekom. (2005). The Environmental Impact Assessment and study (quality and quantity) of the Development Projects in the Lake Uromiyeh Basin, The West Azerbaijan Water Authority (WWA).

Xu, H., 2006. Modification of normalised difference water index (ndwi) to enhance open water features in remotely sensed imagery. Int. J. Remote Sens. 27 (14), 3025–3033. https://doi.org/10.1080/01431160600589179.